

## THE INTRA-CLUSTER MAGNETIC FIELD IN ABELL 401

F. Govoni,<sup>1</sup> K. Dolag,<sup>2</sup> M. Murgia,<sup>1,3</sup> L. Feretti,<sup>3</sup> and S. Schindler<sup>4</sup>

### RESUMEN

Presentamos avances de un trabajo en progreso que apunta al estudio de la magnitud y estructura del campo magnético en el cúmulo caliente de galaxias A401. Con este propósito derivamos la medida de rotación de dos fuentes de radio utilizando el Very Large Array a 3.6 cm y 6 cm. Los datos son interpretados en base a las expectativas de un modelo tridimensional del campo magnético. Se encuentra que un campo magnético multi-escala con una magnitud del orden de 4  $\mu$ G en el centro del cúmulo reproduce las observaciones bastante bien.

### ABSTRACT

We present a work in progress aimed to study the magnetic field strength and structure in the hot cluster of galaxies A401. For this purpose we derived the rotation measure of two cluster radio sources by using Very Large Array observations at 3.6 cm and 6 cm. The data are interpreted on the basis of the expectation of a 3D cluster magnetic field model. A multi-scale magnetic field with a strength of about 4  $\mu$ G at the cluster center reproduces the data quite well.

*Key Words:* galaxies: clusters: general — intergalactic medium — radio continuum: galaxies — X-rays: galaxies: cluster

### 1. INTRODUCTION

The presence of a magnetized plasma between an observer and a radio source changes the properties of the polarized emission from the radio source. Therefore information on clusters magnetic fields along the line-of-sight can be determined, in conjunction with X-ray observations of the hot gas, through the analysis of the Rotation Measure (RM) of radio galaxies in the background or in the galaxy clusters themselves.

Through sensitive, high resolution (3''), VLA polarization observations within 3.6 cm and 6 cm bands, we derived the RM images of two radio galaxies belonging to the cluster of galaxies Abell 401. The analysis of the Faraday rotation of these sources, can be used to constrain the cluster magnetic field properties, by following the approach proposed by Murgia et al. (2004).

### 2. ABELL 401

A401 is a hot ( $T=8.0$  keV), nearby ( $z=0.074$ ) cluster of galaxies characterized by the presence of a radio halo (e.g. Bacchi et al. 2003) around the cD

galaxy at the cluster center. The periphery of the cluster hosts few extended head tail radio galaxies.

Figure 1 shows the 1.4 GHz radio contours of A401 obtained from the NRAO VLA Sky Survey (Condon et al. 1998) overlaid on the Rosat PSPC X-ray image obtained from the Rosat All Sky Survey. In this work we have analyzed those radio galaxies labeled with A401A and A401B.

The source A401A is located to the West of the cluster center at a projected distance of about 5.3'. The high resolution image at 6 cm reveals a peculiar morphology. A compact double structure of about 20'' in size and a low surface brightness tail of about 1.3' in size with a morphology which appears not directly connected to the compact emission. The very steep spectrum tail of this source is likely disconnected from the currently active compact component. Therefore A401A seems a dying radio galaxies which started again its activity.

The head tail A401B is instead located at a projected distance of about 8.8' to the South East of the cluster center with the head pointed versus the South of the cluster and the tail elongated versus the North.

### 3. ROTATION MEASURE IMAGES

The polarized synchrotron radiation incoming from radio sources, undergoes the following rotation of the plane of polarization as it passes through the magnetized and ionized intra-cluster medium

$$\Psi_{\text{Obs}}(\nu) = \Psi_{\text{Int}} + (c/\nu)^2 \times \text{RM}, \quad (1)$$

<sup>1</sup>INAF-Osservatorio Astronomico di Cagliari, Loc. Poggio dei Pini, Strada 54, I-09012 Capoterra (CA), Italy.

<sup>2</sup>Max-Planck-Institut für Astrophysik, Garching, Germany.

<sup>3</sup>INAF-Istituto di Radioastronomia, Via Gobetti 101, I-40129 Bologna, Italy.

<sup>4</sup>Institut für Astrophysik, Leopold-Franzens-Universität Innsbruck, Technikerstraße 25, 6020 Innsbruck, Austria.

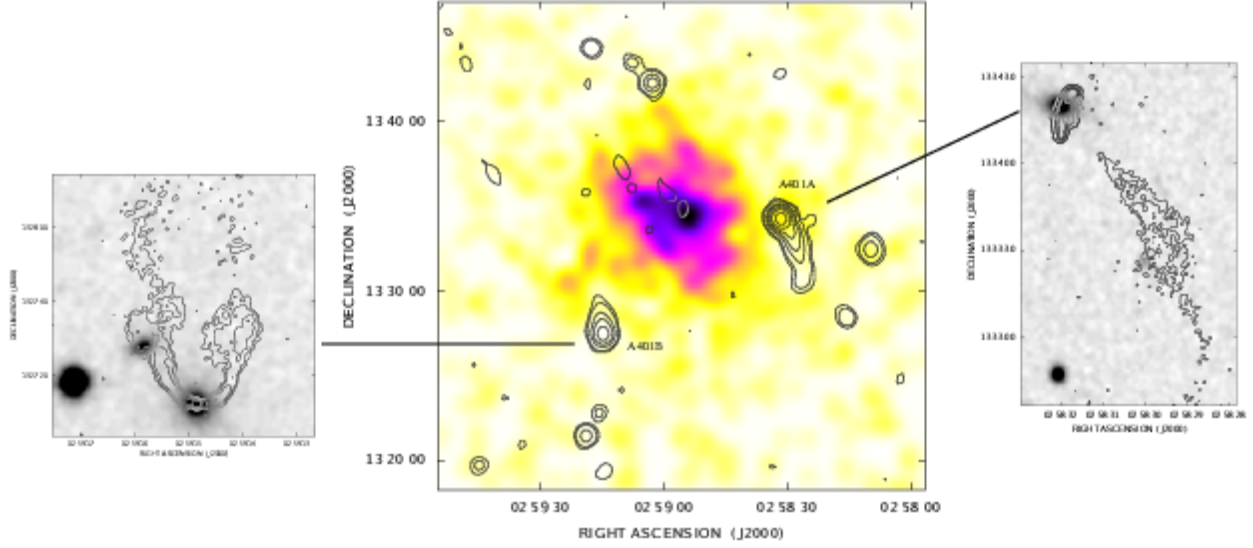


Fig. 1. 1.4 GHz radio image of A401 obtained from the NVSS (contours) overlaid on the *Rosat* X-ray image (colors) in the 0.1–2.4 keV band obtained from the Rosat All Sky Survey. Radio contour levels are: 1.5, 3, 10, 20, 40, 80, 160 mJy/beam. The radio image has an angular resolution of  $45''$ . The sources indicated with the labels A401A and A401B have been analyzed in this work. Higher resolution observations at 6 cm overlaid on the DSS2 red plate of the two radio galaxies are inset.

where  $\Psi_{\text{Obs}}(\nu)$  is the observed polarization angle at a frequency  $\nu$  and  $\Psi_{\text{Int}}$  is the intrinsic polarization angle.

The Rotation measure RM is related to the thermal electron density,  $n_e$ , and magnetic field along the line-of-sight,  $B_{\parallel}$ , through the cluster by the equation:

$$\text{RM} = 812 \int_0^L n_e B_{\parallel} dl \quad \text{rad m}^{-2}, \quad (2)$$

where  $B_{\parallel}$  is measured in  $\mu\text{G}$ ,  $n_e$  in  $\text{cm}^{-3}$  and  $L$  is the depth of the screen in kpc.

The observing strategy to get information on the cluster magnetic field intensity and structure is to obtain high resolution RM maps of sources located in a cluster. If interpreted in terms of an external Faraday screen, the RM values combined with measurements of the thermal gas density can be used to derive information on the magnetic field along line of sights crossing different regions of the cluster.

Figure 2 shows the rotation measure images, at  $3''$  resolution, of the two sources. Following the definition, the Faraday RM images were obtained by performing a fit of the polarization angle images, at each pixel, as a function of  $\nu^{-2}$  (see equation 1) by using the algorithm PACERMAN (Polarization Angle CorrEcting Rotation Measure ANalysis) by Dolag et al. (2005). The images have been obtained by fitting the polarization angle maps  $\Psi_{\text{Obs}}$

at the frequencies 4535, 4885, 8085, and 8465 MHz. Figure 2 (right) shows the histograms of the RM distribution for the sources. We can characterize the obtained RM distribution in terms of a mean ( $\langle \text{RM} \rangle$ ) and root mean square ( $\sigma_{\text{RM}}$ ). For A401A we obtained  $\langle \text{RM} \rangle = +257 \text{ rad/m}^2$  and  $\sigma_{\text{RM}} = 118 \text{ rad/m}^2$  while for A401B we obtained  $\langle \text{RM} \rangle = +116 \text{ rad/m}^2$  and  $\sigma_{\text{RM}} = 82$ . In both the images are evident patchy structures with RM fluctuations down to a scale of few kpc.

In general the RM structures on small scales can be explained by the fact that the cluster magnetic field fluctuates on scales smaller than the size of the sources. On the other hand, in the case in which the RM distribution has a non-zero mean indicate that the magnetic field fluctuates also on scales larger than the radio sources. Therefore, in order to interpret correctly the RM data we have to take into account magnetic field fluctuations in a wide range of spatial scales.

#### 4. STUDY OF THE INTRACLUSTER MAGNETIC FIELD

The software FARADAY (Murgia et al. 2004), by comparing RM observations with 2D and 3D Monte Carlo simulations, permits to analyze the magnetic field power spectrum in clusters of galaxies. We assume that a cluster magnetic field can be described

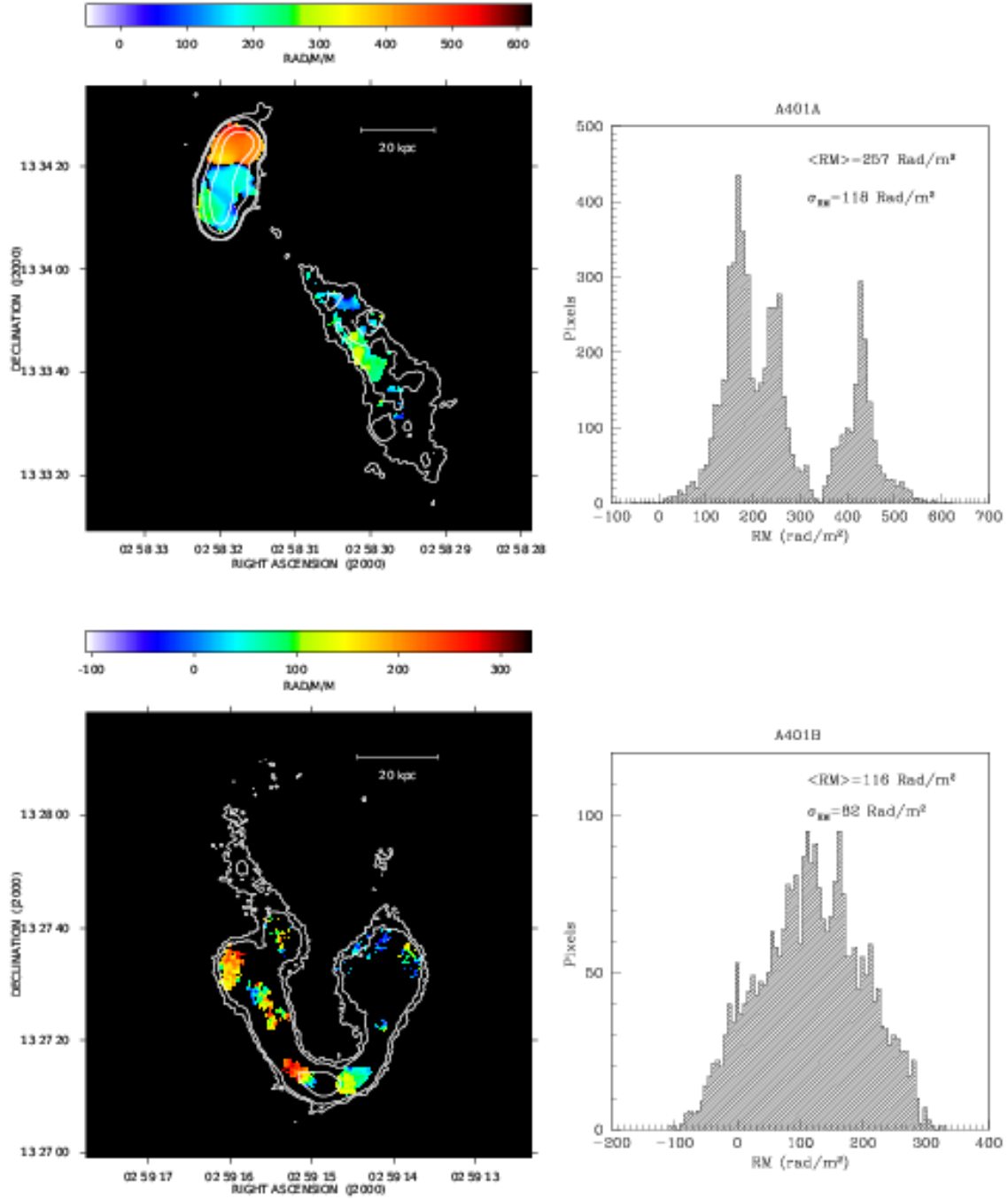


Fig. 2. Rotation measure of the radio galaxies in A401. The angular resolution is  $3''$ . The contours refer to the total intensity images at 3.6 cm. Contours are drawn at  $-0.06, 0.06, 0.12, 1, 5$  mJy/beam. The histograms show the rotation measure distribution for all significant pixels.

by a simple power law power spectrum of the type<sup>5</sup>:

$$|B_k|^2 \propto k^{-n}. \quad (3)$$

<sup>5</sup>Note that the power spectrum is expressed as vectorial form in  $k$ -space. The one-dimensional form can be obtained by multiplying by  $4\pi k^2$  and  $2\pi k$  respectively the three and two-dimensional power spectra. According to this notation the Kolmogorov spectral index is  $n = 11/3$ .

Moreover we consider a magnetic field whose strength decreases from the cluster center according to:

$$\langle \mathbf{B} \rangle(r) = \langle B_0 \rangle \left[ \frac{n_e(r)}{n_0} \right]^\eta. \quad (4)$$

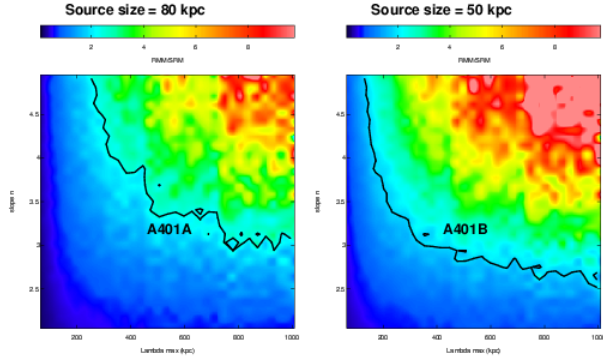


Fig. 3. 2D Simulations of the ratio  $|\langle \text{RM} \rangle|/\sigma_{\text{RM}}$  calculated over the source size, as a function of the magnetic field power spectrum index and the largest scale of the magnetic field fluctuations. In the figures are indicated the values of  $|\langle \text{RM} \rangle|/\sigma_{\text{RM}}$  obtained for the two sources A401A and A401B in comparison with the simulations. It is evident the degeneracy between  $n$  and  $\Lambda_{\text{max}}$ : the different combinations of these two parameters may yield an equally good fit to the RM values.

The adopted magnetic field model has five free parameters:

- average magnetic field strength at the cluster centre ( $\langle B_0 \rangle$ );
- power spectrum spectral index ( $n$ );
- minimum and maximum scale of the magnetic field fluctuations ( $\Lambda_{\text{min}}, \Lambda_{\text{max}}$ );
- magnetic field radial profile slope ( $\eta$ ).

By varying all these parameters we expect synthetic RM images characterized by very different statistics and structure.

It is important to note that there are two main degeneracies between the model parameters (Murgia et al. 2004). The first degeneracy is between  $n$  and  $\Lambda_{\text{max}}$ : the higher is  $n$  the lower is  $\Lambda_{\text{max}}$ . The second one is between  $\eta$  and  $B_0$ : the higher is  $\eta$  the higher is  $B_0$ . This means that different combinations of these parameters may yield an equally good fit to the data.

As shown in Figure 3, 2D simulation of synthetic RM maps permit to evaluate the range of  $n$ - $\Lambda_{\text{max}}$  which give rise to the observed  $|\langle \text{RM} \rangle|/\sigma_{\text{RM}}$ .

Figure 4 shows an example of a 3D magnetic field model which well represents the data for a fixed value of  $n$  and  $\Lambda_{\text{max}}$  as determined on the basis of Figure 3. For example, by fixing  $\eta = 0.3$ , and by considering a Kolmogorov magnetic field power spectrum spectral index  $n=11/3$  and  $\Lambda_{\text{max}} = 250$  kpc, a central magnetic field of about  $4 \mu\text{G}$  explain the data quite

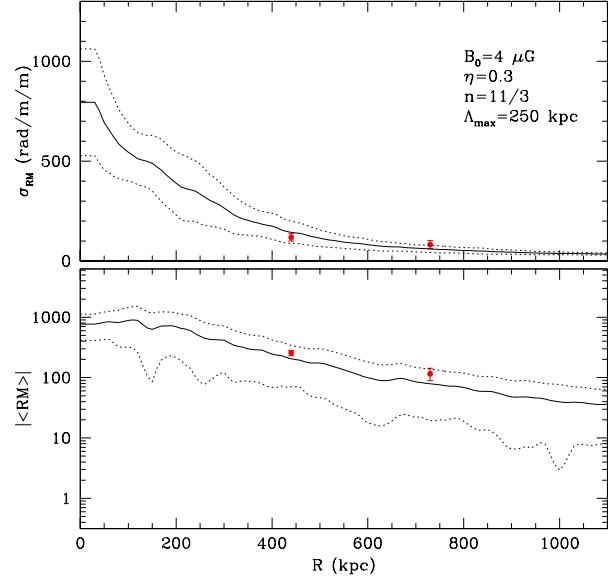


Fig. 4. Example of a 3D magnetic field model which well represents the observed data. A central magnetic field of  $4 \mu\text{G}$  which decrease from the cluster center with  $\eta = 0.3$  explain the data quite well.

well. The analysis to solve the degeneracy between  $n$  and  $\Lambda_{\text{max}}$  is still in progress.

## 5. CONCLUSION

We presented a work in progress aimed to study the magnetic field strength and structure in the hot cluster of galaxies A401. For this purpose we derived the rotation measure of two cluster radio sources. The data are interpreted on the basis of the expectation of a 3D magnetic field model. A multi-scale magnetic field model with a strength of about  $4 \mu\text{G}$  at the cluster center reproduces the data quite well.

This work has been partially funded by the Grant ASI-INAF I/088/06/0 High Energy Astrophysics.

## REFERENCES

- Bacchi, M., Feretti, L., Giovannini, G., & Govoni, F. 2003, *A&A*, 400, 465
- Condon, J. J., et al. 1998, *AJ*, 115, 1693
- Dolag, K., Vogt, C., & Enßlin, T. A. 2005, *MNRAS*, 358, 726
- Murgia, M., Govoni, F., Feretti, L., Giovannini, G., Dallacasa, D., Fanti, R., Taylor, G. B., & Dolag, K. 2004, *A&A*, 424, 429